
[View Journal Online](#)
[View Article Online](#)

Synthesis, crystal structure, Hirshfeld surface and interaction energies analysis of 5-methyl-1,3-bis(3-nitrobenzyl)pyrimidine-2,4(1*H*,3*H*)-dione

 Koffi Senam Etsè ^{1,*}, Laura Comeron Lamela ¹, Guillermo Zaragoza ² and Bernard Pirotte ¹
¹ Laboratory of Medicinal Chemistry, Center for Interdisciplinary Research on Medicines (CIRM), University of Liège, Quartier Hôpital B36 Av. Hippocrate 15 B-4000 Liège, Belgium

ks.etsè@uliege.be (K.S.E.), l.comeron@uliege.be (L.C.L.), b.pirotte@uliege.be (B.P.)

² Unidade de Difracción de Raios X, RIAIDT, Universidade de Santiago de Compostela, Campus VIDA, 15782 Santiago de Compostela, Spain
 g.zaragoza@usc.es (G.Z.)

* Corresponding author at: Laboratory of Medicinal Chemistry, Center for Interdisciplinary Research on Medicines (CIRM), University of Liège, Quartier Hôpital B36 Av. Hippocrate 15 B-4000 Liège, Belgium.

e-mail: ks.etsè@uliege.be (K.S. Etsè).

RESEARCH ARTICLE



doi 10.5155/eurjchem.11.2.91-99.1973

Received: 19 February 2020

Received in revised form: 22 March 2020

Accepted: 24 March 2020

Published online: 30 June 2020

Printed: 30 June 2020

KEYWORDS

 Thymine
 Crystal structure
 Hirshfeld surfaces
 Hydrogen bonding
 Interaction energies
 3-Nitrobenzylbromide

ABSTRACT

The title compound 5-methyl-1,3-bis(3-nitrobenzyl)pyrimidine-2,4(1*H*,3*H*)-dione was obtained by reaction of thymine with 3-nitrobenzylbromide in the presence of cesium carbonate. Characterization of the product was achieved by NMR spectroscopy and its stability was probed in basic condition using UV-Visible analysis. Furthermore, the molecular structure was confirmed by X-ray diffraction analysis. The compound crystallizes in orthorhombic *Pna*21 space group with unit cell parameters $a = 14.9594$ (15) Å, $b = 25.711$ (3) Å, $c = 4.5004$ (4) Å, $V = 1731.0$ (3) Å³ and $Z = 4$. The crystal packing of the title compound is stabilized by intermolecular hydrogen bond, $\pi \cdots \pi$ and C-H \cdots π stacking interactions. The intermolecular interactions were furthermore analyzed through the mapping of different Hirshfeld surfaces. The two-dimensional fingerprint revealed that the most important contributions to these surfaces come from O \cdots H (37.1%), H \cdots H (24%) and H \cdots C/C \cdots H (22.6%) interactions. The interaction energies stabilizing the crystal packing were calculated and were presented graphically as framework energy diagrams. Finally, the energy-framework analysis reveals that $\pi \cdots \pi$ and C-H \cdots π interactions energies are mainly dispersive and are the most important forces in the crystal.

 Cite this: *Eur. J. Chem.* 2020, 11(2), 91-99

 Journal website: www.eurjchem.com

1. Introduction

Heterocyclic compounds containing the pyrimidine ring has wide occurrence in nature [1]. Together with adenine, guanine, cytosine, and uracil, thymine is one of the fundamental nitrogenous bases observed in the genetic code of the living beings. As nucleobase, thymine is implicated in various important biological processes [2]. Numerous thymine derivatives are described as biologically active compounds. Some of them are reported as efficient to inhibit the highly invasive A431 tumor cell line [3], active against the majority of wild-type of human immunodeficiency HIV-1 mutant viruses [4], inhibitory potency on a mycobacterial enzyme thymidine mono-phosphate kinase (TMPKmt), on the growth of *M. smegmatis* and *M. tuberculosis* bacteria [5], susceptibility to phosphorylation by TK1 and TK2 and candidates for application as boron carriers for boron neutron capture therapy (BNCT) [6]. Among the various substituted thymine derivatives, the *N*¹,*N*³-benzyl substituted compounds are recognized to be interesting according to their conformation and the rigidity offered by the different rings. In particular,

nitrobenzyl-substituted pyrimidine derivatives show potency in agrochemical field as herbicides [7], in the medical and pharmaceutical fields as bio-reductive alkylating agents [8] or even as anti-epileptogenic agents [9,10] and photosensitizer for the photodynamic therapy [11].

Our group is continuously interested in the synthesis, full characterization and evaluation of biological activity of benzoisothiazoles [12] and benzothiadiazines as AMPA receptor antagonist [13-15]. As a part of our works, we recently became interested in the synthesis of new structures based on the thymine heterocycle such as Willardiine [16] derivatives containing the nitrobenzyl substituent. Although some 1,3-bis(nitrobenzyl)thymine compounds are described [8], their molecular structures obtained by X-ray diffraction analysis were not reported at all. In view to develop new family of these interesting compounds, various key precursors are prepared. Herein, we report, the synthesis, the crystal structure, the Hirshfeld surface analysis and the interaction energies of 5-methyl-1,3-bis(3-nitrobenzyl)pyrimidine-2,4(1*H*,3*H*)-dione.

Table 1. Crystal data and details of the structure refinement for title compound.

Parameters	Compound
Empirical formula	C ₁₉ H ₁₆ N ₄ O ₆
Formula weight	396.36
Temperature (K)	100(2)
Crystal system	Orthorhombic
Space group	<i>Pna</i> 2 ₁
a (Å)	14.9594(15)
b (Å)	25.711(3)
c (Å)	4.5004(4)
Volume (Å ³)	1731.0(3)
Z	4
ρ _{calc} (g/cm ³)	1.521
μ (mm ⁻¹)	0.116
F(000)	824.0
Crystal size (mm ³)	0.10 × 0.06 × 0.03
Radiation	MoKα (λ = 0.71073)
2θ range for data collection (°)	5.446 to 56.568
Index ranges	-19 ≤ h ≤ 19 -34 ≤ k ≤ 34 -5 ≤ l ≤ 6
Tmin, Tmax (sin θ/λ) max (Å ⁻¹)	0.911, 0.953 0.667
Reflections collected	78246
Independent reflections	4257 [R _{int} = 0.0736, R _{sigma} = 0.0265]
Data/restraints/parameters	4257/1/263
Goodness-of-fit on F ²	1.068
Final R indexes [I ≥ 2σ (I)]	R ₁ = 0.0367, wR ₂ = 0.0833
Final R indexes [all data]	R ₁ = 0.0447, wR ₂ = 0.0883
Largest diff. peak/hole (e Å ⁻³)	0.21/-0.22
Flack parameter	-0.1(4)

2. Experimental

All the chemicals and solvents used were of analytical grade from Sigma Aldrich or Abcr. Melting points were determined on a Büchi Tottoli capillary apparatus and are uncorrected. The ¹H and ¹³C NMR spectra were recorded on a Bruker Avance (500 MHz for ¹H; 125 MHz for ¹³C) instrument using deuterated dimethyl sulfoxide (DMSO-*d*₆) as the solvent with tetramethylsilane (TMS) as an internal standard; chemical shifts are reported in δ values (ppm) relative to that of internal TMS. The abbreviations s = singlet, d = doublet, t = triplet, q = quadruplet, m = multiplet, dd = doublet of doublet, qd = quadruplet of doublet, dt = doublet of triplet, tt = triplet of triplet, and bs = broad singlet are used throughout. Elemental analyses (C, H, N, S) were realized on a Thermo Scientific Flash EA 1112 elemental analyzer and were within ±0.4% of the theoretical values for carbon, hydrogen, and nitrogen. This analytical method certified a purity of ≥95% for each tested compound. All reactions were routinely checked by TLC on silica gel Merck 60F₂₅₄ [17].

2.1. Synthesis of 5-methyl-1,3-bis(3-nitrobenzyl)pyrimidine-2,4(1H,3H)-dione

In a 50 mL one-neck round-bottomed flask equipped with a magnetic bar containing thymine (1 g, 7.93 mmol, 1 equiv.), 3-nitrobenzylbromide (3.44 g, 15.86 mmol, 2 equiv.) and cesium carbonate (3.41 g, 10.46 mmol, 1.3 equiv.), was added 30 mL of dry dimethylformamide. The mixture was stirred at 30 °C for 3 days. At the end of the reaction, the excess of Cs₂CO₃ was eliminated by filtration and the solution was diluted with 200 mL of water. The desired compound was extracted with ethyl acetate. The organic fraction was dried over MgSO₄ and the solvent was removed under vacuum. The light-yellow powder was purified by silica-gel column chromatography using an ethyl acetate as eluent giving the desired product. Color: White powder. Yield: 90%. R_f (ethyl acetate): 0.77. M.p.: 152-154 °C. UV/Vis (DMSO, λ_{max}, nm): 271. Anal. calcd. for C₁₉H₁₆N₄O₆: C, 57.58; H, 4.07; N, 14.14. Found: C, 57.55; H, 4.31; N, 13.97 %. ¹H NMR (500 MHz, DMSO-*d*₆, δ, ppm): 8.20-8.16 (m, 2H, Ar-*H*), 8.13-8.10 (m, 2H, Ar-*H*), 7.88 (d, 1H, *J* = 1 Hz, C=C-*H*-N), 7.79 (d, 1H, *J* = 5 Hz, Ar-*H*), 7.73 (d, 1H, *J* = 5 Hz, Ar-*H*), 7.66 (t, 1H, *J* = 7.5 Hz, Ar-*H*), 7.61 (t, 1H, *J* =

7.5 Hz, Ar-*H*), 5.13 (s, 2H, N-CH₂), 5.06 (s, 2H, N-CH₂), 1.85 (s, 3H, CH₃). ¹³C NMR (126 MHz, DMSO-*d*₆, δ, ppm): 162.92, 151.11, 147.77, 147.64, 140.38, 139.21, 138.79, 34.34, 134.16, 130.13, 129.85, 122.61, 122.29, 122.22, 122.19, 108.50, 50.83, 43.21, 12.51.

2.2. Crystal growth

Monocrystal of the title compound 5-methyl-1,3-bis(3-nitrobenzyl)pyrimidine-2,4(1H,3H)-dione was obtained by slow evaporation at 6 °C of its solution in a 1:1 mixture of acetone and dichloromethane.

2.3. Single crystal X-ray diffraction data collection

For the crystal structure determination, the data were collected by applying the omega and phi scans method on a Bruker D8 Venture PHOTON III-14 diffractometer using INCOATEC multilayer mirror monochromated with MoKα radiation (λ = 0.71073 Å) from a microfocus sealed tube source at 100 K. Computing data and reduction were made with the APEX3 [18]. The structure was solved using SHELXT [19] and finally refined by full-matrix least-squares based on F² by SHELXL [20]. An empirical absorption correction was applied using the SADABS program. Software used to molecular graphics: ORTEP for Windows [21]. Software used to prepare material for publication: WinGX publication routines [21] and Mercury [22].

Crystal data, data collection and structure refinement details are summarized in Table 1. All non-hydrogen atoms were refined anisotropically and the hydrogen atom positions were included in the model on the basis of Fourier difference electron density maps. All CH and aromatic CH hydrogen (C-H = 0.95 Å) atoms were refined using a riding model with U_{iso}(H) = 1.2 U_{eq}(C). The methyl hydrogen (C-H = 0.99 Å) atoms were refined as a rigid group with torsional freedom [U_{iso}(H) = 1.5 U_{eq}(C)].

3. Results and discussion

3.1. Synthesis and UV-visible

The title product was obtained by reacting thymine and 3-

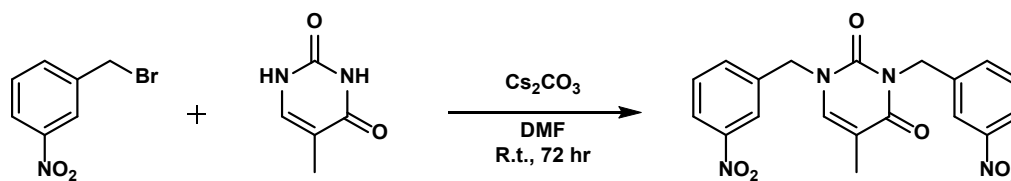


Figure 1. Synthesis of 5-methyl-1,3-bis(3-nitrobenzyl)pyrimidine-2,4(1H,3H)-dione.

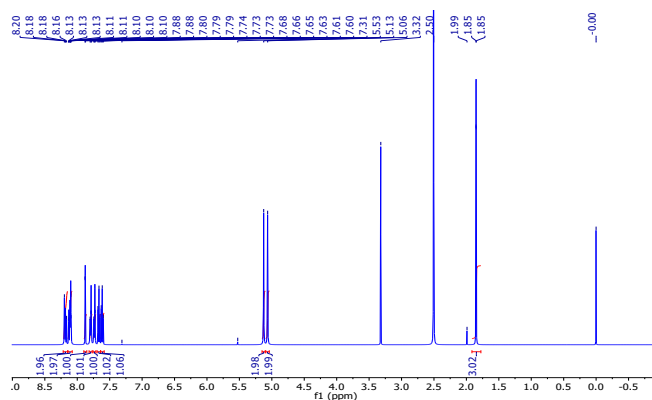


Figure 2. ^1H NMR (500 MHz) spectrum of 5-methyl-1,3-bis(3-nitrobenzyl)pyrimidine-2,4(1H,3H)-dione in $\text{DMSO}-d_6$ at 298 K.

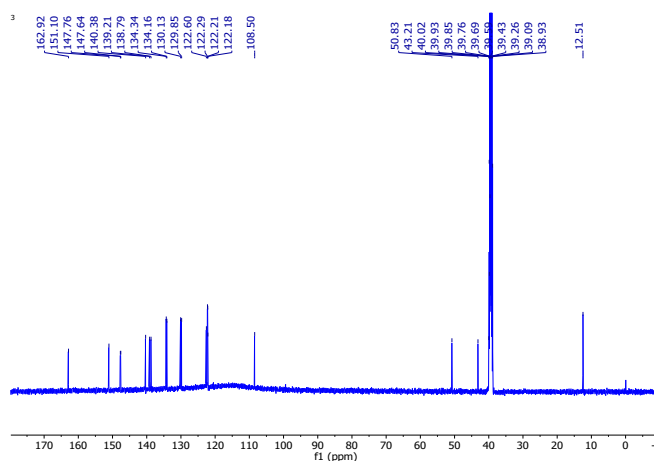


Figure 3. ^{13}C NMR (126 MHz) spectrum of 5-methyl-1,3-bis(3-nitrobenzyl)pyrimidine-2,4(1H,3H)-dione in $\text{DMSO}-d_6$ at 298 K.

nitrobenzyl bromide in the presence of cesium carbonate as base in dry dimethylformamide as shown in Figure 1. The desired product was isolated as a white powder after silica-gel column chromatography and characterized by NMR.

The proton NMR spectrum of the product is shown in Figure 2. This spectrum highlights one singlet at δ 1.85 ppm easily attributed to the methyl CH_3 group and two singlets at δ 5.13 and 5.06 ppm corresponding to the two different benzyl CH_2 hydrogens. Furthermore, the endocyclic CH hydrogen of the heterocycle can be recognized by the peak at δ 7.8 ppm. Finally, the set of peaks between δ 7.6 and 8.2 ppm, can be attributed to hydrogens of the aromatic rings.

The ^{13}C NMR spectrum (Figure 3) of the title compound was recorded in $\text{DMSO}-d_6$ at 298 K to complete the nuclear magnetic resonance characterization. The chemical shifts are observed between 180 and -10 ppm. The $-\text{CH}_3$ carbon of the thymine appears at 12.51 ppm. The two benzyl carbons are characterized by two different chemical shifts at 50.83 and 43.21 ppm respectively. This result is logical since the N^1 substituted methylene carbon in 5-methyl-1,3-bis(3-nitrobenzyl)pyrimidine-2,4(1H,3H)-dione located between two carbonyl groups is more deshielded than its counterpart at the

N^3 position. The carbons of the carbonyl groups are observed at 162.92 and 151.11 ppm, respectively.

Characterization of the isolated compound by UV-Visible spectroscopy was also realized. Moreover, the stability of the title compound was investigated in alkaline condition (pH ranging from 7 to 13) using UV/Vis spectroscopy. The absorbance is recorded at room temperature on a HP ChemStation (HP 845X UV-visible Software) with an HP 8453 UV-visible Spectrophotometer (Hewlett Packard, Waldbronn, Germany) fitted with a 1024-element diode-array. Roughly, 100 μM concentration of the compound is used in the experiment and the pH is adjusted using sodium hydroxide and hydrochloride solution. The spectra obtained under neutral pH condition shows a single peak at 271 nm that can be assigned to the $\pi-\pi^*$ transition in the molecule (Figure 4). In contrary to the effect of base on thymine reported by Kaspar *et al.* [23], the results revealed that the alkaline condition does not affect the UV/Vis spectrum of the 1,3-bis(3-nitrobenzyl)thymine (Figure 4). This result is logical because in this product, acidic protons are replaced by benzyl substituents that avoid formation of mesomeric forms (in case of thymine) leading to good stability of the compound.

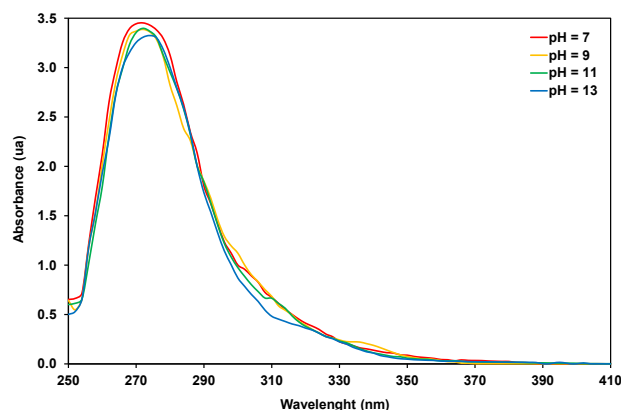


Figure 4. UV/Vis spectra of 5-methyl-1,3-bis(3-nitrobenzyl)pyrimidine-2,4(1H,3H)-dione at pH ranging 7 to 13.

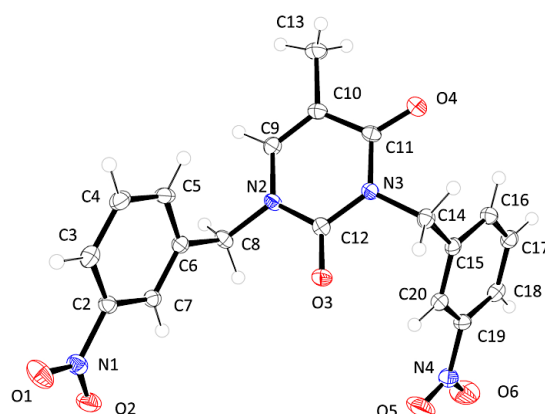


Figure 5. ORTEP diagram for the title compound with displacement ellipsoids drawn at the 50% probability level.

3.2. Molecular structure

To complete the structural characterization, the exact molecular structure of the title compound was obtained by X-ray diffraction analysis. The structure of 5-methyl-1,3-bis(3-nitrobenzyl)pyrimidine-2,4(1H,3H)-dione is shown in Figure 5.

The compound crystallizes in orthorhombic *Pna21* space group. The two nitro bond lengths are identical with C2-N1 and C19-N4 values of 1.472 (3) and 1.470 (3) Å, respectively (Table 2). All the nitro N-O bonds distances are similar (~1.22 Å). Moreover, analysis of the thymine heterocycle highlights close carbonyl C12-O3 and C11-O4 bonds distances with 1.218 (3) and 1.225 (3) Å. The double bond C9-C10 distance [1.344 (3) Å] is typical of those observed in olefin.

The endocyclic C-N bonds of the imide moiety distances are different, especially those of the C12-N2 [1.378 (3) Å], C12-N3 [1.390 (3) Å] and C11-N3 [1.403 (3) Å]. Distortion of the thymine six member ring is observed by measuring selected internal bond angle C9-C10-C11, N2-C12-N3, C12-N2-C9 and C12-N3-C11 giving notable variation with 118.4 (2)°, 115.19 (19)°, 121.79 (17)° and 125.40 (18)°, respectively. The torsion angles C10-C9-N2-C12 [1.2 (4)°] and C10-C11-N3-C12 [1.3 (3)°] are closer and reveal low deviation of the amide bonds from planarity. Furthermore, the weighted average ABS. torsion angle value is 2.7°, suggesting a flattened (planar) conformation of the thymine ring.

3.3. Supramolecular features

The crystal structure packing of the title compound is stabilized by the existence of intermolecular hydrogen bonds.

The H-bond interaction [C14-H14B...O2ⁱ, (i) $x-1/2, -y+1/2, z$] is established between the benzyl hydrogen atom of one molecule and one oxygen atom of the nitro group of an adjacent molecule with distances H14...O2ⁱ of 2.88 Å, C14B...O2ⁱ of 3.453 (3) Å, with an angle C14-H14B...O2ⁱ of 144° (Figure 6a).

The molecular conformation revealed that the two benzyl moieties bearing the thymine heterocycle are in the *trans* disposition with the dihedral angle of 176.23 (8)° (Figure 6b). Such disposition of the benzyl groups allows further stabilization of the crystal packing ensured by $\pi\cdots\pi$ and X-H... π interactions. The $\pi\cdots\pi$ interactions are established between equivalent aromatic rings of neighboring molecules (See Table 3 and Figure 6b) and C8-H8 with the π electrons of the phenyl ring (C2→C7), all of them along *c* axis.

3.4. Hirshfeld surface and fingerprint

Hirshfeld surface representation is recognized as a powerful tool for studying intermolecular interactions and molecular packing trends in crystals. This analysis model was used to evaluate intermolecular interactions of the title compound calculated with the program CrystalExplorer 17 [24]. The normalized contact distance, d_{norm} is obtained by considering the global relation between the distances of any surface point to the nearest interior (d_i) and exterior (d_e) atom and the Van der Waals radii (rvdw) of the atoms [25,26].

The maps of d_{norm} , d_i and d_e on molecular Hirshfeld surfaces of the title compound are shown in Figure 7. The three-dimensional d_{norm} surface mapped over a fixed color - 0.2010 (red) to 1.0774 (blue) highlights intermolecular O...H close contacts as red spots which reveals that the sum of d_i and

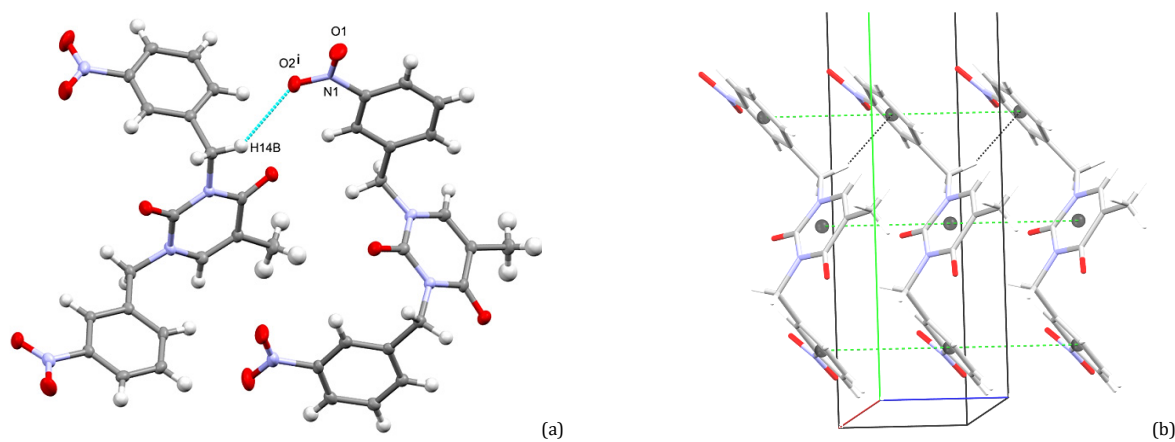
Table 2. Selected bond lengths [Å] and angles [°] for 5-methyl-1,3-bis(3-nitrobenzyl)pyrimidine-2,4(1*H*,3*H*)-dione.

Bond	Distance [Å]	Bond	Angle [°]
C9-C10	1.344 (3)	C12-N2-C9	121.79 (17)
C10-C13	1.497 (3)	C12-N2-C8	117.45 (18)
C10-C11	1.447 (3)	C12-N3-C14	116.34 (18)
C11-O4	1.225 (3)	C11-N3-C14	118.19 (17)
C12-O3	1.218 (3)	C12-N2-C9	121.79 (17)
C2-N1	1.472 (3)	C12-N2-C8	117.45 (18)
C8-N2	1.468 (3)	C12-N3-C14	116.34 (18)
C9-N2	1.381 (3)	C11-N3-C14	118.19 (17)
C11-N3	1.403 (3)	O4-C11-N3	120.60 (2)
C12-N2	1.378 (3)	N3-C11-C10	115.83 (18)
C14-N3	1.478 (3)	C9-N2-C8	120.62 (19)
C19-N4	1.470 (3)	C12-N3-C11	125.40 (18)
C12-N3	1.390 (3)	C9-C10-C11	118.40 (2)
C11-N3	1.403 (3)	O4-C11-C10	123.60 (2)
C12-N2	1.378 (3)	O3-C12-N2	122.13 (19)
C14-N3	1.478 (3)	N2-C12-N3	115.19 (19)
N1-O2	1.225 (3)	O3-C12-N3	122.70 (2)
N4-O6	1.224 (3)	O4-C11-N3-C12	-177.7 (2)
N1-O1	1.225 (3)	N2-C9-C10-C11	3.0 (4)
N4-O5	1.220 (3)	C9-C10-C11-N3	-4.1 (3)
		C10-C9-N2-C12	1.2 (4)
		N2-C12-N3-C11	2.6 (3)
		O3-C12-N2-C9	177.3 (2)
		N3-C12-N2-C9	-3.9 (3)
		O3-C12-N3-C11	-178.7 (2)
		C9-C10-C11-O4	174.9 (2)
		C10-C11-N3-C12	1.3 (3)

Table 3. Analysis of short ring-interactions.

Cg(I)→Cg(I)	Cg-Cg (Å)	Alpha (°)	Beta (°)	Gamma (°)	CgI Perp (Å)	CgI Perp (Å)
Cg1→Cg1 ⁱⁱⁱ	4.5003(14)	0.00(10)	40.6	40.6	3.4188(9)	3.4188(9)
Cg2→Cg2 ⁱⁱⁱ	4.5006(14)	0.02(11)	41.2	41.2	3.3839(9)	3.3840(9)
Cg3→Cg3 ⁱⁱⁱ	4.5005(16)	0.00(12)	40.4	40.4	3.4289(10)	3.4290(10)
Cg(I)→Cg(I)	H-Cg (Å)	H-Perp (Å)	Gamma (Å)	X-H...Cg (°)	X...Cg (Å)	
C8-H8B→Cg2 ⁱ	2.44	-2.42	5.98	156.00	3.365(2)	

ⁱ [x, y, 1+z]; ⁱⁱ [x, y, -1+z]; Cg1 (N2 C9 C10 C11 N3 C12); Cg2 (C2→C7); Cg3 (C15→C20).

**Figure 6.** (a) Intermolecular hydrogen bond. (i) $x-1/2, -y+1/2, z$. (b) Intermolecular interactions in the crystal packing of title compound.

d_e is shorter than the sum of the Van der Waals radii (Figure 7c). White and blue regions on the surface reveal distances equal and longer than the sum of the Van der Waals radii respectively [25]. On the Hirshfeld surface mapped with shape-index, convex blue regions represent hydrogen donor groups and concave red regions represent acceptor groups (Figure 7d).

The electrostatic potentials for 5-methyl-1,3-bis(3-nitrobenzyl)pyrimidine-2,4(1*H*,3*H*)-dione were calculated at B3LYP/6-31G(d,p) level of theory and mapped on the Hirshfeld surfaces (Figure 7e). The map analysis allows a quantitative evaluation of the electron-rich and electron-deficient sites in the molecule. The blue and red regions around the different atoms correspond to positive and negative electrostatic potentials respectively. As shown in Figure 7e, in the molecule, the electronegative regions are

essentially located around the oxygen atoms and the electropositive regions were observed around the C-H bonds.

The dispositions adopted by the molecules in the crystal packing lead to close contacts that could be quantified by the mapping of the two-dimensional fingerprint. The fingerprint plot indicates the contributions of interatomic contacts to the Hirshfeld surfaces of the crystal packing. In 1,3-bis(3-nitrobenzyl)thymine, decomposed fingerprint reveals that the most important contributions come from O...H (37.1%), H...H (24%) and H...C/C...H (22.6%) interactions. The high contribution of O...H contacts in the fingerprint could be explained by the presence of several oxygen atoms in the nitro groups and in the thymine cycle. Other interactions are H...N/N...H (4%), C...O/O...C (3.2%), C...C (2.5%) N...O/O...N (2.1%) and C...N/N...C (0.7%) (Figure 8).

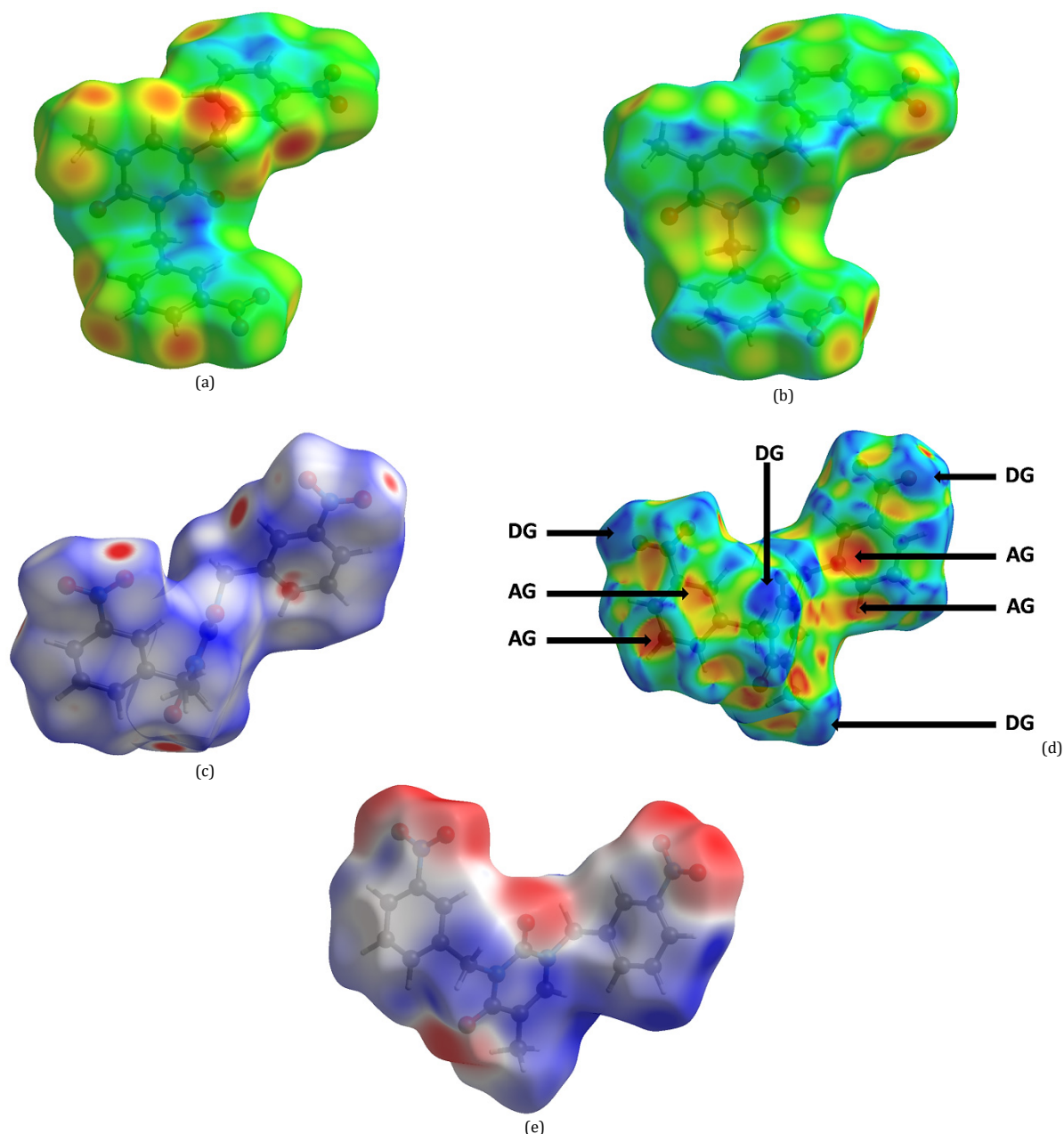


Figure 7. The Hirshfeld surface of the title compound mapped over: (a) d_i in the range 0.9306 to 2.5121 Å, (b) d_e in the range 0.9306 to 2.5121 Å, (c) d_{norm} in the range -0.2010 to 1.0774, (d) shape-index (-1.0 to 1.0, DG: Donor Group, AG: Acceptor Group) and (e) electrostatic potential in the range -0.0646 to 0.043 atomic units.

3.5. Energy framework

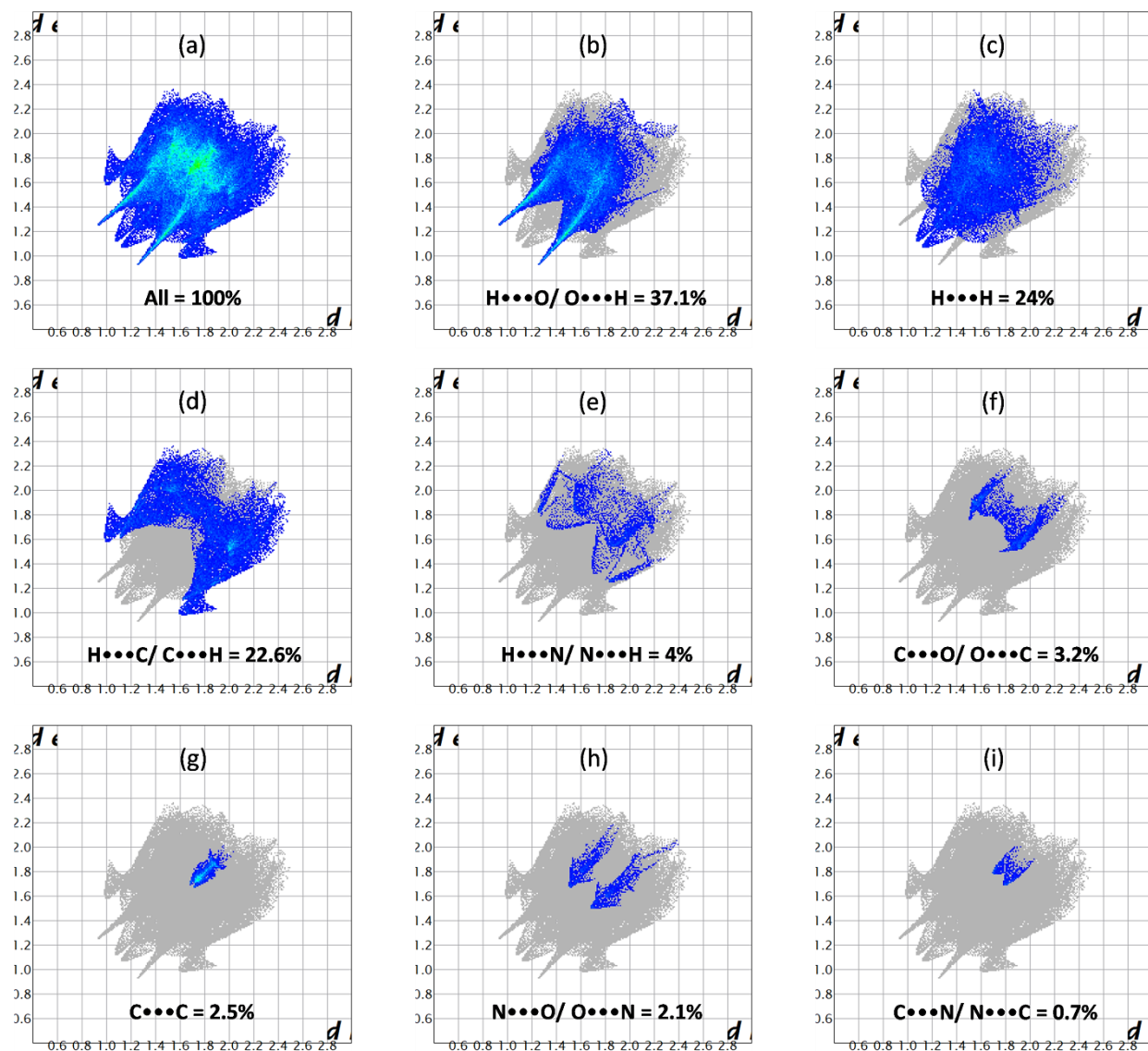
In view to get more accuracy about molecular interactions, we use Tonto quantum chemistry package for wave-function calculation as an alternative to Gaussian16 quantum chemistry packages [27]. The various intermolecular interactions depicted in the title compound participate to the crystal packing stabilization. Therefore, the intermolecular interaction energies for 5-methyl-1,3-bis(3-nitrobenzyl)pyrimidine-2,4(1*H*,3*H*)-dione are calculated using CE-B3LYP/6-31G(d,p) energy model available in Crystal-Explorer (CE) [24].

The interaction energies calculations are represented graphically in Figure 9 as framework energy diagrams. The radii of the corresponding cylinders are proportional to the magnitude of interaction energy. The total intermolecular energy E_{tot} (kJ/mol) relative to the reference molecule (in black) is the sum of energies of four main components,

comprising electrostatic (E_{ele}), polarization (E_{pol}), dispersion (E_{dis}) and exchange-repulsion (E_{rep}) [28] with scale factors of 1.057, 0.740, 0.871 and 0.618, respectively [29,30]. Table 3 shows information about interaction energies components (E), rotational symmetry operations with respect to the reference molecule (Symop), the centroid-to-centroid distance between the reference molecule and interacting molecules (R) as well as the number of pair(s) of interacting molecules with respect to the reference molecule (N). The results give total interaction energy of -199.7 kJ/mol involving the electrostatic (-83.8 kJ/mol), polarization (-29.8 kJ/mol), dispersion (-217.4 kJ/mol) and repulsion (162.4 kJ/mol). The $\pi \cdots \pi$ and C-H \cdots π contacts highlight in Figure 6b are the most stable interactions present in the crystal packing with an interaction energy of -58.5 kJ/mol. Hydrogen bonds with C-H \cdots O interactions energies are in the same energy order with π -X interactions with energy value of -56.3 kJ/mol.

Table 3. Interaction energies in components form for 5-methyl-1,3-bis(3-nitrobenzyl)pyrimidine-2,4(1*H*,3*H*)-dione.

N	Symp	R	E _{ele}	E _{pol}	E _{dis}	E _{rep}	E _{tot}
2	-x+1/2, y+1/2, z+1/2	14.01	-9.4	-2.3	-16.3	9.8	-19.8
2	-x, -y, z+1/2	13.57	-1.0	-0.5	-9.7	6.2	-6.0
2	-x+1/2, y+1/2, z+1/2	15.39	-6.8	-1.7	-5.4	6.3	-9.3
2	x, y, z	4.50	-1.8	-8.6	-104.5	65.9	-58.5
2	-x, -y, z+1/2	12.97	0.1	-1.4	-10.9	6.9	-6.2
2	x+1/2, -y+1/2, z	8.73	-17.2	-3.2	-23.8	16.9	-30.9
2	x+1/2, -y+1/2, z	8.73	-7.0	-1.8	-6.5	2.7	-12.7
2	x+1/2, -y+1/2, z	7.49	-40.7	-10.3	-40.3	47.7	-56.3
Total			-83.8	-29.8	-217.4	162.4	-199.7

**Figure 8.** The two-dimensional fingerprint plots of title compound: (a) all contacts, (b) H...O/O...H, (c) H...H, (d) H...C/C...H, (e) H...N/N...H, (f) C...O/O...C, (g) C...C, (h) N...O/O...N and (i) C...N/N...C.

That interaction energy presents the same order electrostatic ($E'_{ele} = -40.7 \text{ kJ}\cdot\text{mol}^{-1}$) and dispersive ($E'_{dis} = -40.3 \text{ kJ}\cdot\text{mol}^{-1}$) character (Table 3). Analysis of the total energy diagram (Figure 9d) revealed close resemblance to the dispersion energy framework (Figure 9c) demonstrating its main contribution in the total forces in the crystal packing.

4. Conclusion

The reaction of thymine with 3-nitrobenzylbromide in the presence of cesium carbonate yielded 5-methyl-1,3-bis(3-

nitrobenzyl)pyrimidine-2,4(1*H*,3*H*)-dione as a white powder. The NMR and elemental analysis of the product were further completed by X-ray diffraction analysis performed on the isolated monocrystal obtained by slow evaporation. All the interactions present in the crystal packing were analyzed thank to Hirshfeld surface analysis and the two-dimensional fingerprint, highlighting close contacts as well as acceptor and donor groups. Finally, energy-framework calculations were used to analyze and visualize the three dimensional topology of the crystal packing. The results revealed that total interaction energy in the crystal packing is mainly dispersive.

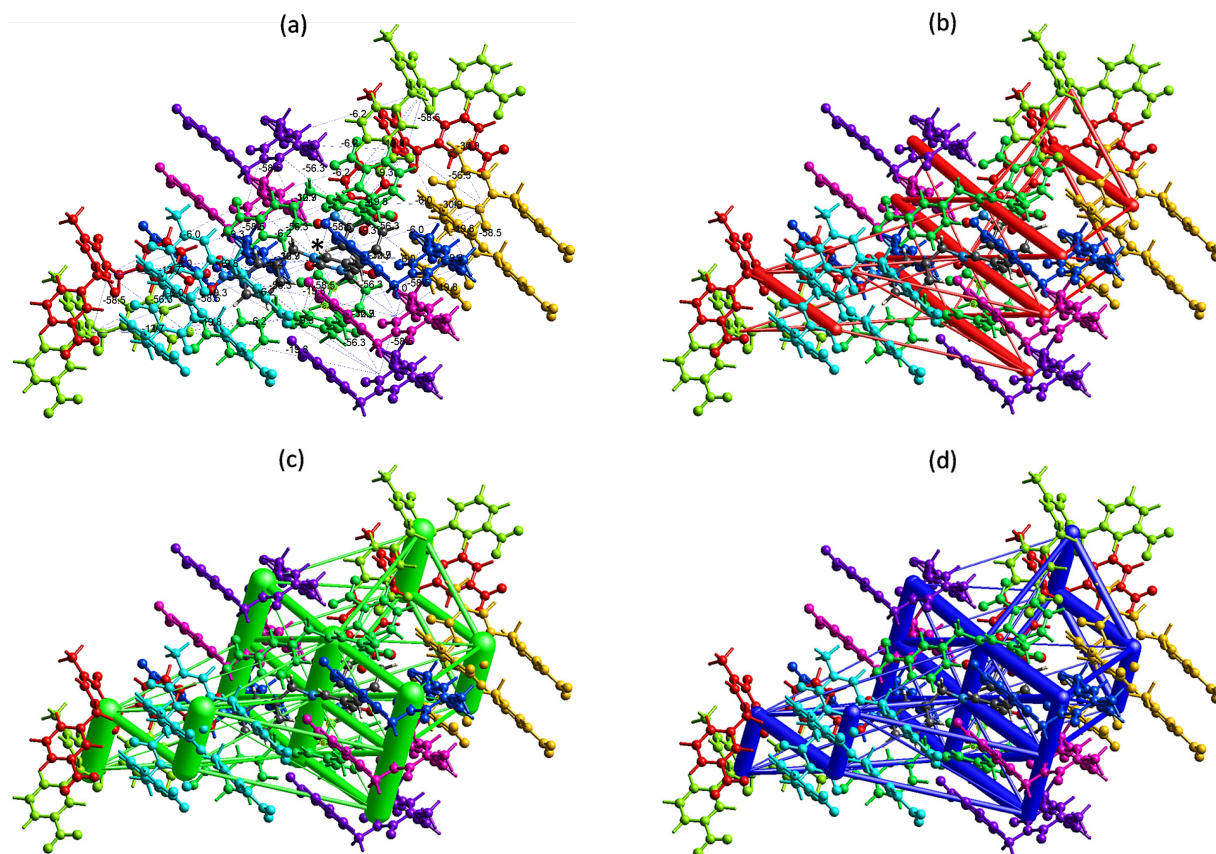


Figure 9. The colour-coded interaction energy framework map of 5-methyl-1,3-bis(3-nitrobenzyl)pyrimidine-2,4(1H,3H)-dione within 3.8 Å of the centering (marked by an asterisk) molecular cluster (a). Energy framework diagram for separate electrostatic (b), dispersion (c) components of the title molecule and the total interaction energy (d). The energy factor scale is 100 and the cut-off is 5.00 kJ/mol.

Acknowledgements

The authors thank the Université de Liège for a research grant.

Supporting information

CCDC-1960980 contains the supplementary crystallographic data for this paper. These data can be obtained free of charge via <https://www.ccdc.cam.ac.uk/structures/>, or by e-mailing data_request@ccdc.cam.ac.uk, or by contacting The Cambridge Crystallographic Data Centre, 12 Union Road, Cambridge CB2 1EZ, UK; fax: +44(0)1223-336033.

Disclosure statement

Conflict of interests: The authors declare that they have no conflict of interest.

Author contributions: All authors contributed equally to this work.

Ethical approval: All ethical guidelines have been adhered.

Sample availability: Samples of the compounds are available from the author.

ORCID

Etsè Koffi Sénam

 <http://orcid.org/0000-0001-8495-4327>

Cameron Lamela Laura

 <http://orcid.org/0000-0002-5940-3002>

Zaragoza Guillermo

 <http://orcid.org/0000-0002-2550-6628>

Pirotte Bernard

 <http://orcid.org/0000-0001-8251-8257>

References

- [1]. Lagoja I. M. *Chem. Biodivers.* **2005**, *2*, 1-50.
- [2]. Honda, T.; Inagawa, H.; Fukushima, M.; Moriyama, A.; Soma, G. *Clin. Chim. Acta.* **2002**, *322*, 59-66.
- [3]. Hadj-Bouazza, A.; Teste, K.; Colombeau, L.; Chaleix, V.; Zerrouki, R.; Kraemer, M.; Sainte Catherine, O. *Nucleosides Nucleotides Nucleic Acids* **2008**, *27*, 439-448.
- [4]. Balzarini, J.; Baba, M.; De Clercq, E. *Antimicrob. Agents Chemother.* **1995**, *39*, 998-1002.
- [5]. Adamska, A.; Rumijowska-Galewicz, A.; Ruszczyńska, A.; Studzińska, M.; Jabłonska, A.; Paradowska, E.; Bulska, E.; Munier-Lehmann, H.; Dziadek, J.; Lesnikowski, Z. J.; Olejniczak, A. B. *Eur. J. Med. Chem.* **2016**, *121*, 71-81.
- [6]. Bialek-Pietras, M.; Olejniczak, A. B.; Paradowski, E.; Studzińska, M.; Jabłonska, A.; Lesnikowski, Z. J. *J. Organomet. Chem.* **2018**, *865*, 166-172.
- [7]. Li, G.; Zhu, Y.; Yang, F.; Yang, H. *Hecheng Huaxue.* **2011**, *19*, 111-114.
- [8]. Lin, T. S.; Wang, L.; Antonini, I.; Cosby, L. A.; Shiba, D. A.; Kirkpatrick, D. L.; Sartorelli, A. C. *J. Med. Chem.* **1986**, *29*, 84-89.
- [9]. Weaver, D. F.; Guillain, B. M.; Carran, J. R.; Jones, K. US Patent. 2002, No. 7, 501, 429 B2.
- [10]. Kim, B. R.; Park, J. Y.; Jeong, H. J.; Kwon, H. J.; Park, S. J.; Lee, I. C.; Ryu, Y. B.; Lee, W. S. *J. Enzyme Inhib. Med. Chem.* **2018**, *33*, 1256-1265.
- [11]. Li, M.; Cai, X.; Zhu, Y.; Liu, K.; Hu, M. *Acta Chim. Sinica (Chinese Edition)* **2011**, *69*, 425-430.
- [12]. Etse, K. S.; Dassonneville, B.; Zaragoza, G.; Demonceau, A. *Tetrahedron Lett.* **2017**, *58*, 789-793.
- [13]. Manos-Turvey, A.; Becker, G.; Francotte, P.; Serrano, M. E.; Luxen, A.; Pirotte, B.; Plenevaux, A.; Lemaire, C. *Chem. Med. Chem.* **2019**, *14*, 788-795.
- [14]. Goffin, E.; Drapier, T.; Larsen, A. P.; Geubelle, P.; Ptak, C. P.; Laulumaa, S.; Rovinskaja, K.; Gilissen, J.; Tullio, P.; Olsen, L.; Frydenvang, K.; Pirotte, B.; Hanson, J.; Oswald, R. E.; Kastrup, J. S.; Francotte, P. *J. Med. Chem.* **2018**, *61*, 1251-1264.

- [15]. Etse, K. S.; Zaragoza, G.; Pirotte, B. *Eur. J. Chem.* **2019**, *10*, 189-194.
- [16]. Dolman, N. P.; More, J. C.; Alt, A.; Knauss, J. L.; Troop, H. M.; Bleakman, D.; Collingridge, G. L.; Jane, D. E. *J. Med. Chem.* **2006**, *49*, 2579-2592.
- [17]. Drapier, T.; Geubelle, P.; Bouckaert, C.; Nielsen, L.; Laulumaa, S.; Goffin, E.; Dilly, S.; Francotte, P.; Hanson, J.; Pochet, L.; Kastrop, J. S.; Pirotte, B. *J. Med. Chem.* **2018**, *61*, 5279-529.
- [18]. Bruker APEX II Bruker AXS Inc., Madison, WI, USA, 2004.
- [19]. Sheldrick, G. M. *Acta Cryst. A* **2015**, *71*, 3-8.
- [20]. Sheldrick, G. M. *Acta Cryst. C* **2015**, *71*, 3-8.
- [21]. Farrugia, L. J. *J. Appl. Cryst.* **2012**, *45*, 849-854.
- [22]. Macrae, C. F.; Bruno, I. J.; Chisholm, J. A.; Edgington, P. R.; McCabe, P.; Pidcock, E.; Rodriguez-Monge, L.; Taylor, R.; Van de Streek, J.; Wood, P. A. *J. Appl. Cryst.* **2008**, *41*, 466-470.
- [23]. Kaspar, K.; Giessmann, R. T.; Krausch, N.; Neubauer, P.; Wagner, A.; Gimpel, M. *Methods Protoc.* **2019**, *2*, 60-72.
- [24]. Turner, M. J.; McKinnon, J. J.; Wolff, S. K.; Grimwood, D. J.; Spackman, P. R.; Jayatilaka, D.; Spackman, M. A. CrystalExplorer17, The University of Western Australia. <http://hirshfeldsurface.net>, 2017.
- [25]. Spackman, M. A.; Jayatilaka, D. *CrystEngComm* **2009**, *11*, 19-32.
- [26]. Demircioglu, Z.; Yesil, A. E.; Altun, M.; Bal-Demirci, T.; Ozdemir, N. *J. Mol. Struct.* **2018**, *1162*, 96-108.
- [27]. Frisch, M. J.; Trucks, G. W.; Schlegel, H. B.; Scuseria, G. E.; Robb, M. A.; Cheeseman, J. R.; Scalmani, G.; Barone, V.; Mennucci, B.; Petersson, G. A.; Nakatsuji, H.; Caricato, M.; Li, X.; Hratchian, H. P.; Izmaylov, A. F.; Bloino, J.; Zheng, G.; Sonnenberg, J. L.; Hada, M.; Ehara, M.; Toyota, K.; Fukuda, R.; Hasegawa, J.; Ishida, M.; Nakajima, T.; Honda, Y.; Kitao, O.; Nakai, H.; Vreven, T.; Montgomery, J. A. Jr.; Peralta, J. E.; Ogliaro, F.; Bearpark, M.; Heyd, J. J.; Brothers, E.; Kudin, K. N.; Staroverov, V. N.; Kobayashi, R.; Normand, J.; Raghavachari, K.; Rendell, A.; Burant, J. C.; Iyengar, S. S.; Tomasi, J.; Cossi, M.; Rega, N.; Millam, J. M.; Klene, M.; Knox, J. E.; Cross, J. B.; Bakken, V.; Adamo, C.; Jaramillo, J.; Gomperts, R.; Stratmann, R. E.; Yazyev, O.; Austin, A. J.; Cammi, R.; Pomelli, C.; Ochterski, J. W.; Martin, R. L.; Morokuma, K.; Zakrzewski, V. G.; Voth, G. A.; Salvador, P.; Dannenberg, J. J.; Dapprich, S.; Daniels, A. D.; Farkas, O.; Foresman, J. B.; Ortiz, J. V.; Cioslowski, J.; Fox, D. J. Gaussian16. Gaussian Inc. Wallingford, Connecticut, USA, 2016.
- [28]. Turner, M. J.; Thomas, S. P.; Shi, M. W.; Jayatilaka, D.; Spackman, M. A. *Chem. Commun.* **2015**, *51*, 3735-3738.
- [29]. Mackenzie, C. F.; Spackman, P. R.; Jayatilaka, D.; Spackman, M. A. *IUCr* **2017**, *4*, 575-587.
- [30]. Tan, S. L.; Jotani, M. M.; Tiekink, E. R. T. *Acta Cryst. E* **2019**, *75*, 308-318.



Copyright © 2020 by Authors. This work is published and licensed by Atlanta Publishing House LLC, Atlanta, GA, USA. The full terms of this license are available at <http://www.eurjchem.com/index.php/eurjchem/pages/view/terms> and incorporate the Creative Commons Attribution-Non Commercial (CC BY NC) (International, v4.0) License (<http://creativecommons.org/licenses/by-nc/4.0>). By accessing the work, you hereby accept the Terms. This is an open access article distributed under the terms and conditions of the CC BY NC License, which permits unrestricted non-commercial use, distribution, and reproduction in any medium, provided the original work is properly cited without any further permission from Atlanta Publishing House LLC (European Journal of Chemistry). No use, distribution or reproduction is permitted which does not comply with these terms. Permissions for commercial use of this work beyond the scope of the License (<http://www.eurjchem.com/index.php/eurjchem/pages/view/terms>) are administered by Atlanta Publishing House LLC (European Journal of Chemistry).